

Mechanistic studies of glutamine synthetase from *Escherichia coli*: Kinetic evidence for two reaction intermediates in biosynthetic reaction*

(fast kinetics/mechanism of catalytic cycle)

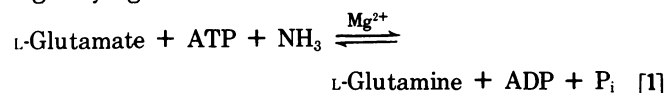
S. G. RHEE AND P. B. CHOCK

Laboratory of Biochemistry, Section of Enzymes, National Heart and Lung Institute, National Institutes of Health, Bethesda, Maryland 20014.

Communicated by E. R. Stadtman, December 8, 1975

ABSTRACT Fast reaction techniques were used to study the kinetics of protein fluorescence intensity changes that are associated with the reactions of unadenylylated *Escherichia coli* glutamine synthetase [L-glutamate: ammonia ligase (ADP-forming), EC 6.3.1.2] with its substrates. It was established that the synthesis of glutamine occurs by a stepwise mechanism. During the catalytic process two fluorometrically distinct intermediates were observed. Both forward and reverse rate constants which lead to the formation and consumption of these intermediates were evaluated. The catalytic rate constant, k_c , which was calculated from these rate constants agrees well with the values of k_c which were determined by direct measurement of the overall biosynthetic activities by means of stopped-flow technique or the steady-state assay method.

Many attempts have been made in recent years (1-4) to elucidate the mechanistic detail of glutamine synthetase (EC 6.3.1.2), a key enzyme in nitrogen metabolism (5). The enzyme from *Escherichia coli* is composed of 12 identical subunits (6) and is known to catalyze several reactions involving the reversible conversion of glutamine to glutamate, glutamine or glutamate to γ -glutamylhydroxamate, and glutamate to pyrrolidone carboxylate (1, 2, 7). Of these reactions, only the biosynthetic reaction (Eq. 1) is known to be physiologically significant.



Despite numerous studies the exact mechanism of this reaction is uncertain. Based mainly on the fact that, in the absence of NH_3 , ATP reacts with L-glutamate to form pyrrolidone carboxylate, ADP, and P_i , and on the fact that the sheep brain enzyme catalyzed the synthesis of ATP from ADP and carbamyl phosphate, Meister and coworkers (3, 7) have suggested that the reaction occurs by a two-step mechanism in which γ -glutamyl phosphate is an intermediate. However, Wedler and Boyer (8) employed isotopic equilibrium kinetic measurements and failed to detect the exchange of $\text{ADP} \rightleftharpoons \text{ATP}$, $\text{P}_i \rightleftharpoons \text{ATP}$, glutamate \rightleftharpoons glutamine, or $\text{NH}_3 \rightleftharpoons$ glutamine unless all substrates are present. On this evidence, they favor a concerted mechanism without the formation of γ -glutamyl phosphate.

Using a fluorometric technique, we have demonstrated (1, 9) that either ATP or L-glutamate can bind independently to the unadenylylated form of the enzyme in the presence of

Mg^{2+} , but when both ATP and L-glutamate are present, a reactive enzyme-bound intermediate is formed instantaneously. With the subsequent addition of NH_3 this reactive intermediate is converted to products. In this paper, we report that two enzyme-bound reactive intermediates are involved in the synthesis of glutamine as catalyzed by Mg^{2+} -activated unadenylylated enzyme.

MATERIALS AND METHODS

Materials. The unadenylylated glutamine synthetase ($\text{E}_{1.0}$)[†] was isolated from *E. coli* grown in a medium containing 35 mM L-glutamate and 0.67 M glycerol. The Mg^{2+} - Zn^{2+} precipitation method (10) as modified by Stadtman (unpublished result) was used for the isolation. In the modified procedure celite is used to trap the precipitated enzyme while one washes out the soluble protein. The precipitated enzyme was then eluted out from the celite matrix with buffer containing no divalent metal ion. Zn^{2+} was removed by dialyzing the enzyme with 2 mM EDTA. The state of adenylation of this enzyme was determined by a method described previously (11). The specific activity of the purified enzyme was determined by a modified procedure developed by Ginsburg *et al.* (12) and the results obtained agree well with the published values for purified enzyme. ATP and L-glutamate were obtained from Sigma Chemical Co. The L-glutamate was contaminated with Ca^{2+} and was purified with Chelex 100 and recrystallization.

Methods. Fluorescence measurements were made using a Hitachi-Perkin-Elmer MPF-2A instrument equipped with a Hewlett-Packard 7004B X-Y recorder and a homemade voltage offset circuit. Constant temperature was maintained using thermostated cell holders and constant temperature circulating baths. The stopped-flow machine used has been described elsewhere (16).

Unless it is specified otherwise, all fluorometric measurements were carried out at 20° and the stopped-flow measurements were performed at 15°. All reactions were carried out in 50 mM *N*-2-hydroxyethylpiperazine-*N'*-2-ethanesulfonic acid (Hepes)-KOH and 0.1 M KCl buffered solution at pH 7.0. Fluorescence emission spectra of the $\text{MgE}_{1.0}$ and the enzyme-substrate complexes were recorded by exciting the tryptophan residues of the enzyme at 300 nm. The emission spectra exhibit a maximum at 336 nm. Special care was taken to remove trace amounts of ammonia in the enzyme (9). All solutions were prepared with freshly redistilled deionized water.

Abbreviation: Hepes, *N*-hydroxyethylpiperazine-*N'*-2-ethanesulfonic acid.

* This paper is Part IV of a series on mechanistic studies of this enzyme. For Part III, see ref. 16.

[†] The subscript indicates the average number of adenylylated subunits per dodecamer.

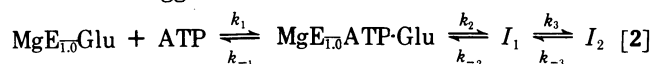
The steady-state assay for the biosynthetic activity is performed by measuring the P_i formed with a method described by Woolfolk *et al.* (6). The reaction was carried out at 15° in the buffer system described above. The concentrations of reactants used are $[ATP] = 5 \text{ mM}$, $[Glu] = 50 \text{ mM}$, $[NH_3] = 50 \text{ mM}$, $[Mg^{2+}] = 20 \text{ mM}$, and $[E_{10}] = 0.13 \text{ } \mu\text{M}$.

The curve-fitting calculations were carried out with the use of an interactive curve-fitting and graphic program, MLAB, developed at the National Institutes of Health and running on a PDP-10 digital computer (13).

RESULTS

Fig. 1 shows a schematic representation of the relationships between time and the changes in protein fluorescence intensity which are associated with the reactions of MgE_{10} and its substrates. A represents the fluorescence intensity increase when a limiting amount of NH_3 , together with an excess of ATP and L-glutamate, is mixed with MgE_{10} . The plateau section between A and C depicts the time required to consume the NH_3 . When NH_3 becomes limiting in the presence of excess ATP and L-glutamate, the high fluorescence intermediate starts to accumulate and it reaches a plateau at C. This high fluorescence intermediate can also be obtained by mixing MgE_{10} with ATP and L-glutamate (broken line E). Regardless of the order of addition, this process is achieved by a time-course which exhibits a nonlinear semilog plot. D depicts the reaction of the high fluorescence intermediate with additional NH_3 .

When MgE_{10} (5.9 μM subunit concentration) is mixed with $MgATP$ (0.6 mM) in the homemade fast mixing cell (16) a very fast change in fluorescence intensity ($t_{1/2} = 1.4 \text{ msec}$) is observed. However, as is shown in Fig. 2B, a relatively slower rate of fluorescence enhancement is obtained when $MgE_{10}Glu$ (i.e., 5.9 μM $E_{10} + 50 \text{ mM}$ glutamate)[†] is mixed with 5 mM ATP. In this case the time-course for the fluorescence enhancement is not a simple exponential function. This is evident from Fig. 2B, which shows a nonlinear first-order plot (curve b). This nonlinear first-order plot is clearly biphasic when the reaction is carried out at lower temperature. However, when a lower concentration of ATP is used, the resulting time-course is less biphasic. These phenomena are due to the facts: (a) that the slower rate is more sensitive to reaction temperature than the fast one; and (b) that the fast rate is a function of the ATP concentration but the slower one is independent of ATP concentration (0.5–5 mM; Rhee, unpublished data). The reaction amplitude is the same whether $MgATP$ is mixed with $MgE_{10}Glu$ or $MgATP$ plus glutamate is mixed with MgE_{10} . A typical oscillogram is shown in Fig. 2B. It is important to point out that a similar type of time-course is also obtained when glutamate is added to $MgE_{10}ATP$. Under these conditions, the amplitude observed is only 56% of that shown in Fig. 2B. The observed time-course suggests a reaction scheme of



[†] Under these conditions, about 70% of the enzyme is in $MgE_{10}Glu$ form. Based on the fact that the same rate and amplitude are also observed when 50 mM Glu and 5 mM ATP are added to MgE_{10} , it indicates that under these conditions Glu must bind very much faster than ATP and the observed fluorescence change is due to the formation of I_1 and I_2 . In addition, the possible interference from the rate of ATP binding to MgE_{10} is negligible since under these conditions, the $t_{1/2}$ for ATP binding is very much less than 1 msec.

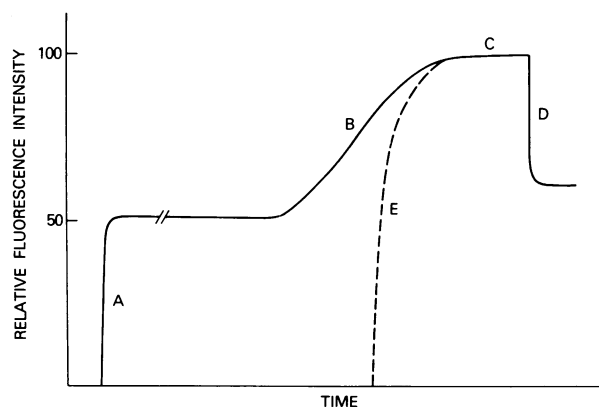


FIG. 1. Schematic representation for the time-course of protein fluorescence changes when substrates are added to MgE_{10} . A, At zero time a limiting amount of NH_3 is added together with an excess ATP and L-glutamate. At B, the ammonia is consumed and accumulation of the high fluorescence $MgE_{10}ATP-Glu$ complex reaches a plateau at C; D shows the results when more NH_3 is added. The broken line is the case when ATP and L-glutamate are added to the MgE_{10} in the absence of NH_3 (E).

where I_1 and I_2 are reaction intermediates 1 and 2, respectively. The fact that only amplitudes are different but not the reaction rates observed due to the order of ATP and glutamate addition indicates that the fluorescence changes induced by I_1 and I_2 formation are very fast relative to the rates of formation of I_1 and I_2 ; therefore, the observed time-course reflects the rates of I_1 and I_2 formed.

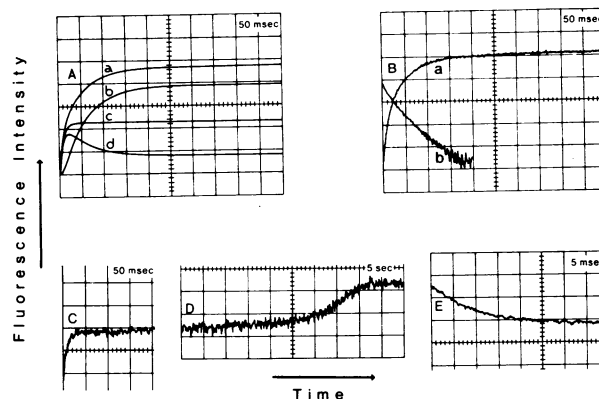


FIG. 2. Computer simulated time-course (A) with $k_2 = 104.1 \text{ sec}^{-1}$, $k_{-2} = 28.8 \text{ sec}^{-1}$, $k_3 = 16 \text{ sec}^{-1}$, and $k_{-3} = 7.06 \text{ sec}^{-1}$ and a relative amplitude of 1.15 and 2.36 V obtained from C and B, respectively (see text). Curve a is the sum of curves b and d; curve b depicts the rate of I_2 formation; curve c shows the rate of I_1 formation when obtained in the presence of NH_4 , ATP, and glutamate; curve d depicts the fate of I_1 . The vertical axis represents the increase of fluorescence intensity at 500 mV per division for all oscillograms shown (except for the first-order plot in B). The enzyme is excited at 300 nm and the emission is recorded at 336 nm. The concentrations of reactants and buffer are $[Mg^{2+}] = 20 \text{ mM}$, $[E_{10}] = 5.9 \text{ } \mu\text{M}$, $[\text{Hepes-KOH}] = 50 \text{ mM}$, $[\text{KCl}] = 0.1 \text{ M}$, $[\text{ATP}] = 5 \text{ mM}$, $[\text{Glu}] = 50 \text{ mM}$, and $[\text{NH}_4] = 0$ (B), 50 mM (C), 1 mM (D), and 5 mM (E). Oscillogram B shows the fluorescence increase (curve a) when $MgATP$ was added to $MgE_{10}Glu$ with a time scale of 50 msec per division and the computer generated semi-log plot (curve b) with a vertical scale of 1.0 per division. (C) Shows the fluorescence increase when $MgATP$ was added to $MgE_{10}Glu-NH_3$. The time scale is 50 msec per division. (D) Shows the time required to consume 1 mM NH_4 and the rise of the high fluorescence species. The time scale is 5 sec per division. (E) shows the fluorescence decrease when NH_4 was added to $MgE_{10}ATP-Glu$. The time scale is 5 msec per division.

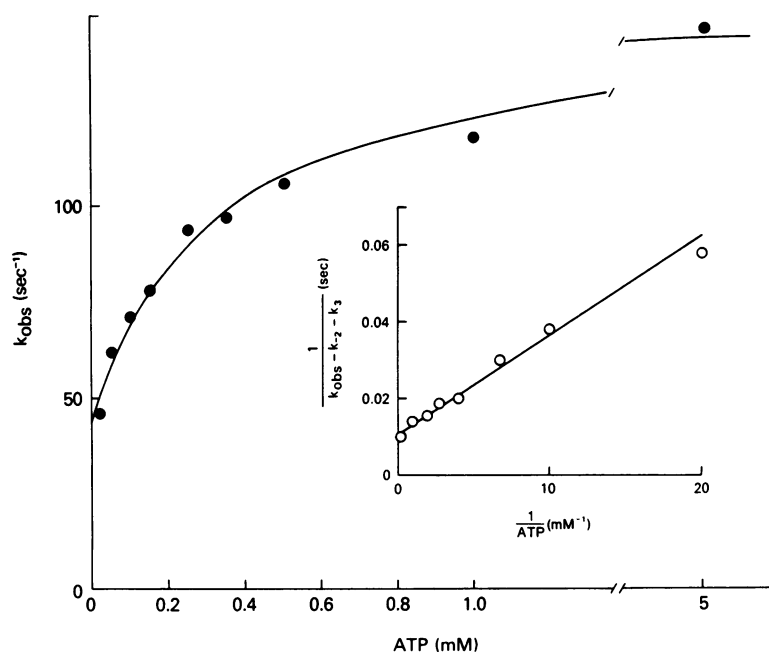


FIG. 3. k_{obs} from the reaction of $\text{MgATP} + \text{MgE}_{1,0}^{\text{Glu-NH}_3}$ plotted as a function of $[\text{ATP}]$. The curve is generated by computer simulation based on Eq. 3 with $K_1 = 3051 \text{ M}^{-1}$, $k_2 = 104.1 \text{ sec}^{-1}$, and $k_{-2} + k_3 = 44.8 \text{ sec}^{-1}$. The dots are experimental data obtained at 15° , pH 7.0, 50 mM Hepes-KOH, 0.1 M KCl, $5 \mu\text{M E}_{1,0}^-$, 50 mM NH_4 , 50 mM L-Glu, and variable $[\text{ATP}]$. The insert is a plot of $(k_{\text{obs}} - k_{-2} - k_3)^{-1}$ versus $[\text{ATP}]^{-1}$ for the same data.

The initial fast reaction rate calculated from the biphasic time-course is essentially the same as the rate obtained when ATP is added to a mixture of $\text{MgE}_{1,0}^-$, glutamate, and ammonia (Fig. 2C). Under these conditions, the slower rate depicted in Fig. 2B is not observed due to the fact that ammonia reacts very rapidly with I_2 , i.e., $k_4 \gg k_{-3}$ (see Discussion). Therefore, the fluorescence change shown in Fig. 2C can be attributed to the formation of I_1 , whose rate of formation is ATP concentration dependent.

However, when $[\text{ATP}]_0 \gg [\text{MgE}_{1,0}^{\text{Glu-NH}_3}]$ (in excess glutamate and NH_3), the data can be treated in accord with Eq. 3, which is derived with the assumption that $\text{MgE}_{1,0}^{\text{Glu}} + \text{ATP} \rightleftharpoons \text{MgE}_{1,0}^{\text{ATP-Glu}}$ is in rapid equilibrium and $[I_2]$ is negligible (see Discussion)

$$k_{\text{obs}} = \frac{k_2}{1 + (K_1[\text{ATP}]_0)^{-1}} + k_{-2} + k_3 \quad [3]$$

where $K_1 = (k_1/k_{-1})$. A computer-simulated curve based on Eq. 3 is given in Fig. 3. With the rearrangement of Eq. 3 a linear plot is obtained when $(k_{\text{obs}} - k_{-2} - k_3)^{-1}$ is plotted against $[\text{ATP}]_0^{-1}$ as shown in the insert of Fig. 3. The constants obtained from these data are $K_1 = 3051 \text{ M}^{-1}$, $k_2 = 104.1 \text{ sec}^{-1}$, and $k_{-2} + k_3 = 44.8 \text{ sec}^{-1}$. The value of $k_2 + k_{-2} + k_3$ can also be obtained by different order of substrate addition. In this case, 50 mM glutamate was added to $\text{MgE}_{1,0}^{\text{ATP-NH}_3}$. The observed amplitude is relatively small

shown in Fig. 2B is due to the sum of the fluorescence levels of intermediates 1 and 2, it is possible to evaluate all the rate constants in reaction 2. When the concentration of ATP is so high that the rate is no longer $[\text{ATP}]$ dependent, such as the case in Fig. 2B, the rate observed is simply the rate of equilibration between $\text{MgE}_{1,0}^{\text{ATP-Glu}}$, I_1 , and I_2 . Utilizing the values for K_1 , k_2 , and $k_{-2} + k_3$ evaluated above, the rate constants k_{-2} , k_3 , and k_{-3} are calculated by computer iteration with Eq. 4 and 5. These equations are derived from a sequential reversible expression (14) with the assumption that the observed amplitude 1 is reflecting the formation of I_1 , since the concentration of I_2 is negligible due to the rapid decomposition of I_2 under the experimental conditions.

$$\text{Amp 1} = 1.15 (k_2 + k_{-2})$$

$$\times \left[\frac{k_{-3}}{\alpha_1 \alpha_2} + \frac{k_{-3} - \alpha_1}{\alpha_1 (\alpha_1 - \alpha_2)} e^{-\alpha_1 t} + \frac{k_{-3} - \alpha_2}{\alpha_2 (\alpha_2 - \alpha_1)} e^{-\alpha_2 t} \right] \quad [4]$$

$$\text{Amp 2} = [2.36 \alpha_1 \alpha_2 - 1.15 k_{-3} (k_2 + k_{-2})]$$

$$\times \left[\frac{1}{\alpha_1 \alpha_2} + \frac{1}{\alpha_1 (\alpha_1 - \alpha_2)} e^{-\alpha_1 t} + \frac{1}{\alpha_2 (\alpha_2 - \alpha_1)} e^{-\alpha_2 t} \right] \quad [5]$$

where Amp 1 and Amp 2 are expected amplitudes due to the formation of I_1 and I_2 , respectively; the values 1.15 and 2.36 are relative fluorescence (in terms of volts) from Fig. 2C and B, respectively, and

$$\alpha_{1,2} = \frac{(k_2 + k_3 + k_{-2} + k_{-3}) \pm \sqrt{(k_2 - k_3 + k_{-2} - k_{-3})^2 + 4k_{-2}k_3}}{2}$$

for this reaction; nevertheless, within the experimental error range, the sum $k_2 + k_{-2} + k_3$, estimated to be $120 \pm 30 \text{ sec}^{-1}$, is in reasonable agreement with the value obtained (148.9 sec^{-1}) from Fig. 3.

With the assumption that the total fluorescence change

The observed amplitude is the sum of Amp 1 and Amp 2. The rate constants so evaluated are $k_2 = 104.1$, $k_{-2} = 28.8$, $k_3 = 16.0$, and $k_{-3} = 7.06 \text{ sec}^{-1}$.

Fig. 2D depicts the rate for the consumption of NH_3 when $[\text{NH}_4]_0$ is relatively low (e.g., $[\text{NH}_4]_0 < 0.5 \text{ mM}$), such

that product inhibition is insignificant, the value of k_c , the catalytic constant, can be estimated to be 6.5 sec^{-1} . Fig. 2E shows the rate of I_2 consumption when 1 mM of NH_4 was added to a solution containing 20 mM Mg^{2+} , $5.9 \mu\text{M}$ $\text{E}_{1,0}^-$, 5 mM ATP, and 50 mM glutamate.

Incidentally, when ATP is added to $\text{MgE}_{1,0}^-$ with or without the presence of glutamate, a very slow fluorescence increase ($t_{1/2} \geq 1 \text{ sec}$) was observed. This reaction is disregarded in this report, since it is too slow to be involved in the catalytic cycle and it is not detected in the presence of NH_3 .

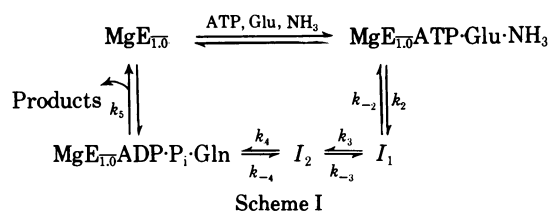
DISCUSSION

To confirm the validity of the rate constants, k_2 , k_{-2} , k_3 , and k_{-3} , calculated on the basis of reaction 2, these rate constants were used to generate time-course by computer simulation. The results are given in Fig. 2A. Curve d in Fig. 2A depicts the fate of I_1 when excess ATP (5 mM) is reacted with $\text{MgE}_{1,0}^-$ or excess ATP and glutamate (50 mM) are added to $\text{MgE}_{1,0}^-$. The rate of I_1 formation is shown in curve c. This rate can be detected when ATP is added to a mixture containing $\text{MgE}_{1,0}^-$ and excess glutamate and NH_4 (50 mM), since under these conditions no I_2 accumulation occurs because of the relatively slow rate of I_2 formation and the rapid rate for the reaction between NH_3 and I_2 . This rationale is further supported by a computer calculation using Scheme I, with all the calculated rate constants and the relative amplitudes exhibited by I_1 and I_2 (not shown). The results are in good agreement with curve c. The steady-state concentration of I_2 is 11% of the total enzyme used. Curve b depicts the rate of I_2 formation and curve a, which is obtained by summing curve b and d, is the expected fluorescence change due to I_1 and I_2 formation. Comparison of curve a and c with the experimental time-course shown in Fig. 2B and C gives excellent agreement.

It is noteworthy that the reaction amplitude observed for the glutamate and $\text{MgE}_{1,0}^-$ reaction is only 56% of that observed when ATP or ATP plus glutamate reacts with $\text{MgE}_{1,0}^-$ or $\text{MgE}_{1,0}^-$, respectively. However, when ATP is added to $\text{MgE}_{1,0}^-$, the amplitude of fluorescence change is much less than the expected value based on fluorescence titration data. This is due to the fact that the reaction rate is

rate constants are evaluated to be 97.8 and 36.2 sec^{-1} for k_4 and k_{-4} (see Scheme I), respectively. When NH_4 concentration is limited in the reaction mixture, time for the consumption of NH_3 can be measured by the increase in fluorescence due to the accumulation of I_2 . It is proportional to NH_4 concentration and inversely proportional to $\text{MgE}_{1,0}^-$ concentration (Rhee, unpublished data). The k_c obtained by this method (6.5 sec^{-1}) is in excellent agreement with that evaluated from P_i measurement (7.2 sec^{-1}) under steady-state assay conditions.

The data obtained here and those reported previously (1, 9, 16) suggest that the catalytic cycle of glutamine biosynthesis when catalyzed by the Mg^{2+} -supported unadenylylated enzyme can be described as:



It is assumed that substrates bind randomly and rapidly (15) and that the release of products is also a rapid step (16). The assumption of a random substrate addition mechanism as shown in Scheme I is based on the facts that: (i) There are synergistic effects observed in the binding of ATP and glutamate as disclosed by fluorescence titrations (9) and by equilibrium isotope exchange kinetics (4). (ii) The total fluorescence enhancement due to ATP binding can be seen only when ATP is added to $\text{MgE}_{1,0}^-$ Glu; this indicates that glutamate can bind to the enzyme prior to ATP. (iii) NH_3 can bind to $\text{MgE}_{1,0}^-$ ATP and produce a stronger fluorescence enhancement for L-alanine binding (Rhee, unpublished data). (iv) Fluorescence enhancement is observed when NH_3 is bound to the $\text{CaE}_{1,0}^-$ Glu (Rhee and Werth, unpublished data).

With the evaluated rate constants reported and the value of 100 sec^{-1} for k_5 estimated from ADP binding study with $\text{MgE}_{1,0}^- \text{P}_i$ (16), k_c is calculated with Eq. 6 to be 8.2 sec^{-1} .

$$k_c = \frac{k_2 k_3 k_4 k_5}{(k_2 k_3 + k_2 k_{-3} + k_{-2} k_{-3})(k_{-4} + k_5) + k_4(k_2 k_3 + k_2 k_5 + k_3 k_5 + k_{-2} k_5)} \quad [6]$$

too fast compared to the dead-time of the stopped-flow machine. Therefore, a significant amount of fluorescence change has taken place before one can record the signal change. The data suggest that when glutamate is bound to the enzyme it retards the rate of ATP-induced protein fluorescence change. When both ATP (5 mM) and glutamate (50 mM) are added simultaneously to $\text{MgE}_{1,0}^-$, glutamate will bind to the enzyme much faster than ATP because it is present at a relatively greater concentration. Therefore, the observed amplitude is the same as that obtained when ATP is added to $\text{MgE}_{1,0}^-$ Glu. This observation and the fact that ATP is known to bind to the enzyme in the absence of glutamate (1) are consistent with a substrate random binding mechanism.

Fig. 2E shows the time-course for the reaction between NH_3 and the highly fluorescence species I_2 . This rate is NH_4 -concentration-dependent (Rhee, unpublished data) and under the experimental conditions described here the

This is in reasonable agreement with the value of 7.2 sec^{-1} obtained from steady-state assay conditions. If I_2 is removed from Scheme I, the rate-limiting step for the catalytic cycle would be k_2 , since the observed amplitude in Fig. 2C is constant until NH_4 is being used up and I_2 is starting to accumulate. With this assumption, k_c calculated would be larger than 30 sec^{-1} , which is clearly not true since the data in Fig. 2D indicate that k_c is 6.2 sec^{-1} . Therefore, I_2 must be involved in the mechanism when NH_4^+ is present.

In essence, we have demonstrated a stepwise mechanism, which involves two intermediates, I_1 and I_2 , for the catalytic cycle in the synthesis of glutamine when Mg^{2+} -supported unadenylylated glutamine synthetase is used as a catalyst.

We wish to thank Dr. E. R. Stadtman for helpful discussion and his critical review of this manuscript. Assistance from D. Towne and G. D. Knott in computer analysis is greatly appreciated.

1. Rhee, S. G., Chock, P. B. & Stadtman, E. R. (1976) *Biochemie*, in press.
2. Stadtman, E. R. & Ginsburg, A. (1974) in *The Enzymes*, ed. Boyer, P. D. (Academic Press, New York), Vol. X, pp. 755-807.
3. Meister, A. (1974) in *The Enzymes*, ed. Boyer, P. D. (Academic Press, New York), Vol. X, pp. 699-754.
4. Wedler, F. C. (1974) *J. Biol. Chem.* **249**, 5080-5087.
5. Stadtman, E. R. (1973) in *The Enzymes of Glutamine Metabolism*, eds. Prusiner, S. & Stadtman, E. R. (Academic Press, New York), pp. 1-6.
6. Woolfolk, C. A., Shapiro, B. M. & Stadtman, E. R. (1966) *Arch. Biochem. Biophys.* **116**, 177-192.
7. Weisbrod, R. E. & Meister, A. (1973) *J. Biol. Chem.* **248**, 3997-4002.
8. Wedler, F. C. & Boyer, P. D. (1972) *J. Biol. Chem.* **247**, 984-992.
9. Timmons, R. B., Rhee, S. G., Luterman, D. L. & Chock, P. B. (1974) *Biochemistry* **13**, 4479-4485.
10. Miller, R. E., Shelton, E. & Stadtman, E. R. (1974) *Arch. Biochem. Biophys.* **163**, 155-171.
11. Shapiro, B. M. & Stadtman, E. R. (1970) in *Methods in Enzymology*, eds. Tabor, H. & Tabor, C. W. (Academic Press, New York), Vol. 17A, pp. 910-922.
12. Ginsburg, A., Yeh, J., Hennig, S. B. & Denton, M. D. (1970) *Biochemistry* **9**, 633-648.
13. Knott, G. D. & Reece, D. K. (1971) *Modellab Users Documentation* (Division of Computer Research and Technology Report, September 1971, National Institutes of Health, Bethesda, Md.).
14. Rodiguin, N. M. & Rodiguin, E. N. (1964) in *Consecutive Chemical Reactions, Mathematical Analysis and Development* (D. Van Nostrand Co., Inc., New York), pp. 42-43.
15. Eigen, M. & Hammes, G. (1963) *Adv. Enzymol.* **25**, 1-38.
16. Rhee, S. G. & Chock, P. B. (1976) *Biochemistry* **15**, in press.